

The Age-Regulating Protein Klotho Is Vital to Sustain Retinal Function

Nicholas J. Reish,¹ Astha Maltare,¹ Alex S. McKeown,² Ann M. Laszczyk,¹ Timothy W. Kraft,² Alecia K. Gross,^{1,2} and Gwendalyn D. King¹

¹Department of Neurobiology, University of Alabama at Birmingham, Birmingham, Alabama

²Department of Vision Science, University of Alabama at Birmingham, Birmingham, Alabama

Correspondence: Alecia K. Gross, University of Alabama at Birmingham, Departments of Vision Science and Neurobiology, 1825 University Boulevard, Shelby 906, Birmingham, AL 35294-2182; agross@uab.edu.

Gwendalyn D. King, University of Alabama at Birmingham, Department of Neurobiology, 1825 University Boulevard, Shelby 913, Birmingham, AL 35294-2182; gdking@uab.edu.

NJR and AM contributed equally to the work presented here and should therefore be regarded as equivalent authors.

Submitted: June 5, 2013

Accepted: September 4, 2013

Citation: Reish NJ, Maltare A, McKeown AS, et al. The age-regulating protein klotho is vital to sustain retinal function. *Invest Ophthalmol Vis Sci*. 2013;54:6675–6685. DOI:10.1167/iov.13-12550

PURPOSE. To determine whether the age-regulating protein klotho was expressed in the retina and determine whether the absence of klotho affected retinal function.

METHODS. Immunohistochemistry and qPCR of klotho knockout and wild-type mice were used to detect klotho expression in retina. Immunohistochemistry was used to probe for differences in expression of proteins important in synaptic function, retinal structure, and ionic flux. Electroretinography (ERG) was conducted on animals across lifespan to determine whether decreased klotho expression affects retinal function.

RESULTS. Klotho mRNA and protein were detected in the wild-type mouse retina, with protein present in all nuclear layers. Over the short lifespan of the knockout mouse (~8 weeks), no overt photoreceptor cell loss was observed, however, function was progressively impaired. At 3 weeks of age neither protein expression levels (synaptophysin and glutamic acid decarboxylase [GAD67]) nor retinal function were distinguishable from wild-type controls. However, by 7 weeks of age expression of synaptophysin, glial fibrillary acidic protein (GFAP), and transient receptor potential cation channel subfamily member 1 (TRPM1) decreased while GAD67, post synaptic density 95 (PSD95), and wheat germ agglutinin staining, representative of glycoprotein sialic acid residues, were increased relative to wild-type mice. Accompanying these changes, profound functional deficits were observed as both ERG a-wave and b-wave amplitudes compared with wild-type controls.

CONCLUSIONS. Klotho is expressed in the retina and is important for healthy retinal function. Although the mechanisms for the observed abnormalities are not known, they are consistent with the accelerating aging phenotype seen in other tissues.

Keywords: aging, protein expression, knockout

The klotho (kl) protein is found to both shorten and extend lifespan depending on its level of expression. In mice, overexpression of kl extends lifespan approximately 30% and confers increased resistance to oxidative stress.^{1,2} Conversely, the absence of kl dramatically reduces lifespan to approximately 8 weeks and induces the development of an array of disorders, typically associated with advanced human age.³ In humans, major alterations in *kl* gene expression are inconsistent with healthy life^{4,5} and minor polymorphic variants are associated with altered risk of disease development.⁶ The kl protein decreases across species and organ systems during normal aging, making it an age-modulating protein that is age-downregulated.⁷

The *kl* gene was detected when a transgene meant to overexpress a sodium-proton exchanger incorrectly inserted into the kl promoter disrupting kl transcription.³ The resulting animal did not express the exchanger, but induced a severe hypomorphic allele for kl. Consistent with a severe hypomorph, RT-PCR amplifies low level mRNA expression but the protein is not detected.^{3,8} In mice, kl functions as both a transmembrane and shed protein. In the kidney, the transmembrane form is critical in maintaining proper ion homeostasis through its role as an FGF23 coreceptor with FGF receptor (FGFR).¹ The shed protein functions throughout the body inhibiting signaling pathways

(wnt, insulin/IGF1, and TGFβ) and altering ion channel function as a weak sialidase.^{9–12} Although the kidney expresses kl the most highly, a few other organs, including the brain, express kl.^{3,13} In the kl knockout, the brain develops a prematurely aged phenotype by 8 weeks of life that includes dysregulation of synaptic protein expression, increases in markers of oxidative stress, apoptosis and autophagy, degeneration of neurons, and cognitive impairment.^{14–18} Together these studies would indicate that kl is important in organs that are sensitive to damage from oxidative stress and that rely on synaptic plasticity for proper function.

We sought to determine whether kl is expressed in the retina and if changes in kl expression level lead to retinal dysfunction or degeneration. Electroretinogram (ERG) was used to assess retinal function in kl knockout mice. We found that the absence of the protein attenuated retinal signaling, while causing either up or downregulation in the expression of key proteins involved in retinal structure and function.

METHODS

Animals

Klotho knockout (129S1/SvImJ) mice were obtained from M. Kuro-o (University of Texas Southwestern, Dallas, TX). The knockout was originally described by Kuro-o.³ Animals were

housed in standard conditions with free access to food and water including Bacon Softies (BioServ, Frenchtown, NJ) or Gel-Diet (Clear H₂O, Portland, ME) as health declined. The whole eye or retina was removed from deeply anesthetized mice at 3 or 7 weeks of age. All procedures were conducted in accordance with the ARVO Statement for the Use of Animals in Ophthalmic and Vision Research using protocols approved by the University of Alabama at Birmingham (UAB) Institutional Animal Care and Use Committee.

Tissue Processing

Retina was flash frozen and stored at -80°C until use. The whole eye was fixed in 4% paraformaldehyde (PFA) and cryoprotected in 30% sucrose prior to freezing in isopentane in preparation for cryosectioning (12- μm slices). To process kidneys, animals were transcardially perfused with tyrode solution (137 mM NaCl, 2.7 mM KCl, 1 mM MgCl₂, 1.8 mM CaCl₂, 0.2 mM Na₂HPO₄, 12 mM NaHCO₃, and 5.5 mM glucose) followed by fixation in PFA and paraffin embedding.

PCR

RNA was extracted from isolated retinas using the RNeasy kit (Qiagen, Valencia, CA). Control human kidney total mRNA was obtained commercially (Clontech, Mountain View, CA). Reverse transcription using iScript RT Supermix and Taqman qPCR using SsoFast Probes Supermix (BioRad, Hercules, CA) were performed per manufacturer's instructions. Primer/probes specific to either mouse 18S ribosomal subunit (MM.PT.49.3175696.g) or mouse kl (Mm.PT.49.11505558) were synthesized by Integrated DNA Technologies (Coralville, IA). For each sample, kl expression was normalized to 18S expression in the sample and compared with control, wild-type kidney kl expression level. Fold change was calculated as $2^{-\Delta\Delta\text{Ct}}$.

Immunohistochemistry (IHC)

Optimal cutting temperature was removed in PBS. Paraffin was removed by sequential incubation in Citrisolv (Fisher, Waltham, MA), isopropanol, and rehydrated in running distilled water. Antigen retrieval in 10 mM citrate buffer was performed in a rice cooker. Slides were allowed to slowly cool to room temperature, washed in PBS, and endogenous peroxidases inactivated in 0.3% H₂O₂. Eye sections were then permeabilized in PBS with 0.5% Triton X100 (PBST) and blocked (1% bovine serum albumin [BSA], 0.2% nonfat milk and 0.3% Triton X100 in PBS). Eye sections were incubated in the following primary antibodies: Synaptophysin (1:250, ab52636; Abcam, Cambridge, MA), post synaptic density 95 (PSD95, 1:1000, ab8258; Abcam), glutamic acid decarboxylase (GAD67, 1:500, g5419; Sigma-Aldrich, St. Louis, MO), sodium potassium ATPase (1:200, ab767; Abcam), glial fibrillary acidic protein (GFAP, 1:500, z033429; Dako, Glostrup, Denmark), transient receptor potential cation channel subfamily member 1 (TRPM1, neat supernatant, gift from T. Wensel; Baylor College of Medicine, Houston, TX), FGF receptor-1 (FGFR1, 1:100, SC121; Santa Cruz, Dallas, TX), SOD-1 (1:500, ab13498; Abcam), Thy1.2 (1:500, ab22489; Abcam), active-caspase 3 (1:1000, 9661; Cell Signaling, Danvers, MA), total caspase 3 (1:1000, 9662; Cell Signaling), HO-1 (1:100, ab13248; Abcam), or Calbindin D-28K (1:250, AB1778; Millipore, Billerica, MA). Primary antibody was detected with relevant secondary antibodies labeled with Alexa594 (Life Technologies, Grand Island, NY). Nuclei were detected by 4',6-diamidino-2-phenylindole (DAPI) and sections mounted in Prolong Gold anti-fade mounting media (Life Technologies).

For wheat germ agglutinin (WGA), sections were incubated in PBS containing DAPI and Alexa555-WGA (Life Technologies) for 10 minutes. Klotho was detected by incubation in primary antibody (1:20, AF1819; R&D Systems, Minneapolis, MN), followed by incubation in ImmPRESS anti-goat IgG peroxidase (Vector Labs, Burlingame, CA) and Cy3-TSA Plus (1:400; PerkinElmer, Waltham, MA). Confocal images were captured on a Zeiss laser scanning LSM710 with a 63 \times , NA 1.4 oil-immersion objective (Zeiss, Peabody, MA).

Intensity Measurement

Slides were imaged on an Olympus BX53 fluorescent microscope using 20 \times objective (Olympus, Center Valley, PA). Intensity measurements performed using Olympus CellSens Dimension 1.7 image analysis software (Olympus). Fluorescent images were taken at identical exposure for wild-type and knockout samples, converted to grayscale format, and identical areas of intensity measured. Intensity measurements were averaged within genotype. For WGA and Thy1.2, images were obtained using a Zeiss LSM510 Meta microscope with a 63 \times objective (Zeiss). The inner plexiform layer (IPL) was outlined in ImageJ (National Institutes of Health, Bethesda, MD) and the average pixel intensity measured. Calbindin expression was quantified by counting the number of positive cells in a 140- μm section of outer plexiform layer (OPL). Statistical significance was determined using GraphPad Prism software and the Student's *t*-test (GraphPad, La Jolla, CA).

Morphometric Analysis

Fresh frozen whole eyes were cryosectioned and slices through the optic nerve head stained with hematoxylin and eosin. Slides were dehydrated in ethanol and xylene and mounted using Permount mounting media (Fisher). Outer nuclear layer thickness was measured using CellSens software (Olympus). The retinal thickness was measured along the vertical meridian in 100- μm increments from the optic nerve head. Lengths at each position were averaged across genotype and statistical significance between groups determined by Student's *t*-test.

Western Blotting

Retina from 7-week-old wild-type and kl knockout mouse was isolated immediately after euthanization, flash frozen, and stored at -80°C until use. Retinal proteins were isolated by sonication in radio immunoprecipitation assay buffer containing DNase (5 $\mu\text{g}/\text{mL}$) and protease inhibitors without EDTA (Pierce, Rockford, IL). Protein concentration was determined by BCA assay, per manufacturer's instructions (Pierce). Ten micrograms of total protein were loaded onto 10% to 12% polyacrylamide gels. Following transfer to nitrocellulose membranes (Fisher), non-specific binding was blocked by incubation in 5% nonfat dry milk in Tris-buffered saline with Triton X100. Primary antibodies were incubated overnight at 4 $^{\circ}\text{C}$ with gentle agitation. In addition to primary antibodies noted above, we utilized actin (1:500; Sigma-Aldrich), α -tubulin (1:500; Life Technologies), rhodopsin (purified 1D4, 0.1 $\mu\text{g}/\text{mL}$), transducin (1:2000, SC-389; Santa Cruz Biotechnology, Santa Cruz, CA), and rhodopsin kinase (1:1000, MA1-720; Pierce). Binding of secondary antibodies conjugated to horse radish peroxidase was detected using chemiluminescent reagents by exposure to film. For quantification, individual band intensity was measured using ImageJ. Each band was normalized to its relevant loading control.

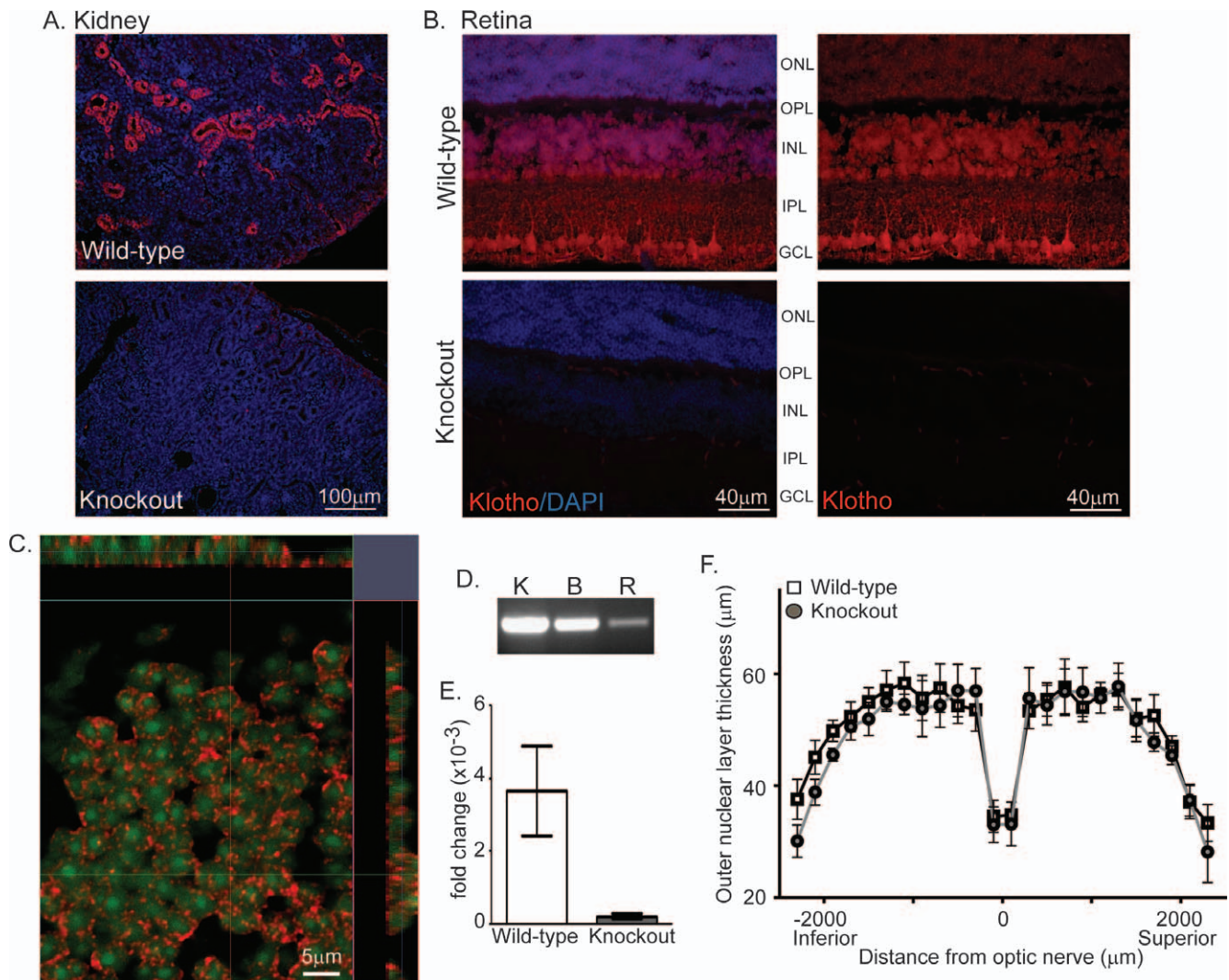


FIGURE 1. Klotho is expressed in retina. (A) Representative images of *kl* protein expression detected by AF1819 in wild-type but not knockout mouse kidney. Nuclei (blue) detected by DAPI. (B) Representative images of *kl* protein expression (red) by detected by AF1819 in wild-type but not knockout mouse retina. Nuclei detected by DAPI. (C) Confocal microscopy with orthogonal projections to detect klotho protein expression (red) and DAPI (represented as pseudo color green, nucleus) in a single optical section (0.35 μm) from the INL of a wild-type retina. (D) Endpoint PCR product detected on ethidium bromide stained gels indicating relative expression levels of *kl* mRNA in wild-type mouse kidney (K), brain (B), and retina (R). (E) The fold change of *kl* mRNA expression in wild-type and knockout mouse retina. Messenger RNA was isolated from retina and kidney and expression level measured by Taqman qPCR. Fold change calculated as $2^{-\Delta\Delta Ct}$ as discussed in methods. (F) Morphometric analysis at 7 weeks of age revealed no evidence of degeneration in *kl* knockout retina as outer nuclear layer thickness was indistinguishable from wild-type retina. ($n = 6$ per group, \pm SEM). OS, outer segment; IS, inner segment.

Electrophysiology

Mice were dark-adapted for at least 4 hours and anesthetized with tribromoethanol (1.25% solution in 150 mM NaCl from a stock solution of 1 g/mL 2,2,2-tribromoethanol in tert-amyl alcohol; Sigma-Aldrich). Following general anesthesia, animals were placed on a heating pad, corneas were anesthetized with proparacaine (0.5%), and pupils dilated with topical phenylephrine HCl (2.5%) and tropicamide (1%). Electroretinogram recordings were collected using a HMsERG unit (Ocuscience, Rolla, MO) and custom loop electrodes of 37-gauge platinum wire (Amazon.com, Seattle, WA). A custom protocol was used with the HMsERG to record scotopic and photopic ERGs over a range of flash intensities (0.01–30 $\text{cd}\cdot\text{s}\cdot\text{m}^{-2}$). ERGView software (Ocuscience) was used to analyze the ERG recordings and determine a- and b-wave amplitudes and latencies.

Selected representative recordings were exported to text file and regraphed in Origin (Originlab, Northampton, MA). To analyze the effects of genotype across flash intensity and time, repeated-measures ANOVAs were performed with the Greenhouse-Geisser correction, using n equals 8 wild-type and n equals 5 knockouts for scotopic ERGs, and $n = 9$ wild-type and $n = 6$ knockouts for photopic data (SPSS software; IBM, Armonk, NY).

RESULTS

kl is Expressed in the Retina

To determine whether *kl* expression is detected in retina, we performed IHC simultaneously on kidney and retinal sections from wild-type and knockout mouse (Figs. 1A–C). Kidney

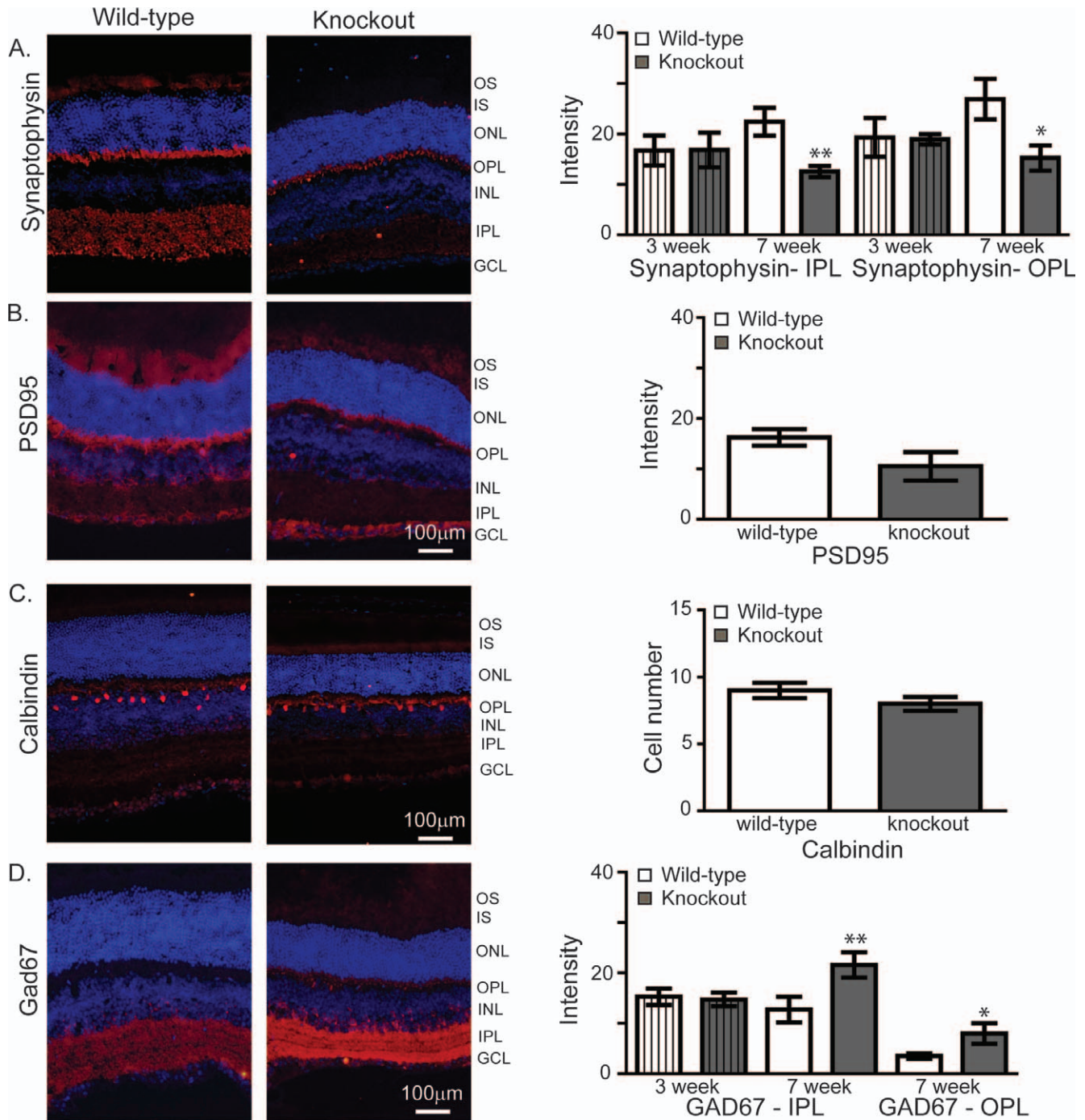


FIGURE 2. In the absence of kl, synaptic proteins are altered by 7 weeks of age. All IHC representative images are from 7-week-old wild-type or knockout mouse retina. *White bars* denote wild-type and *grey bars* denote knockout quantification. (A) Representative synaptophysin IHC images and quantification. Quantification of synaptophysin signal in IPL and OPL was conducted across multiple retinas at 3 weeks (*striped bars*) and 7 weeks (*solid bars*) ($n = 4-5$ per group, \pm SEM, significance determined by Student's *t*-test: * $P < 0.01$, ** $P < 0.005$). (B) Representative PSD95 IHC images and quantification. Quantification detected no significant differences at 7 weeks ($n = 5$ per group, \pm SEM). (C) Representative calbindin IHC images and quantification. Quantification of calbindin positive cell number was conducted across multiple retinas at 7 weeks ($n = 6$ per group, \pm SEM). (D) Representative GAD67 IHC images and quantification. Quantification of GAD67 signal in IPL was conducted across multiple retinas at 3 weeks (*striped bars*) and 7 weeks (*solid bars*) ($n = 5$ per group, \pm SEM, significance determined by Student's *t*-test: * $P < 0.02$).

tissue served as our IHC control as kl is highly expressed in convoluted tubules³ and is completely absent in kl knockouts (Fig. 1A). Klotho was detected in wild-type, but not knockout mouse retina (Fig. 1B). Klotho retinal expression was detected in increasing intensity in the outer nuclear layer (ONL), inner

nuclear layer (INL), and most strongly in the ganglion cell layer (GCL) (Fig. 1B). As expression was concentrated in nuclear layers, we used confocal fluorescent microscopy to determine whether kl was localized in the nucleus as reported in brain.¹⁹ Orthogonal projections from a single plane of the INL reveal kl

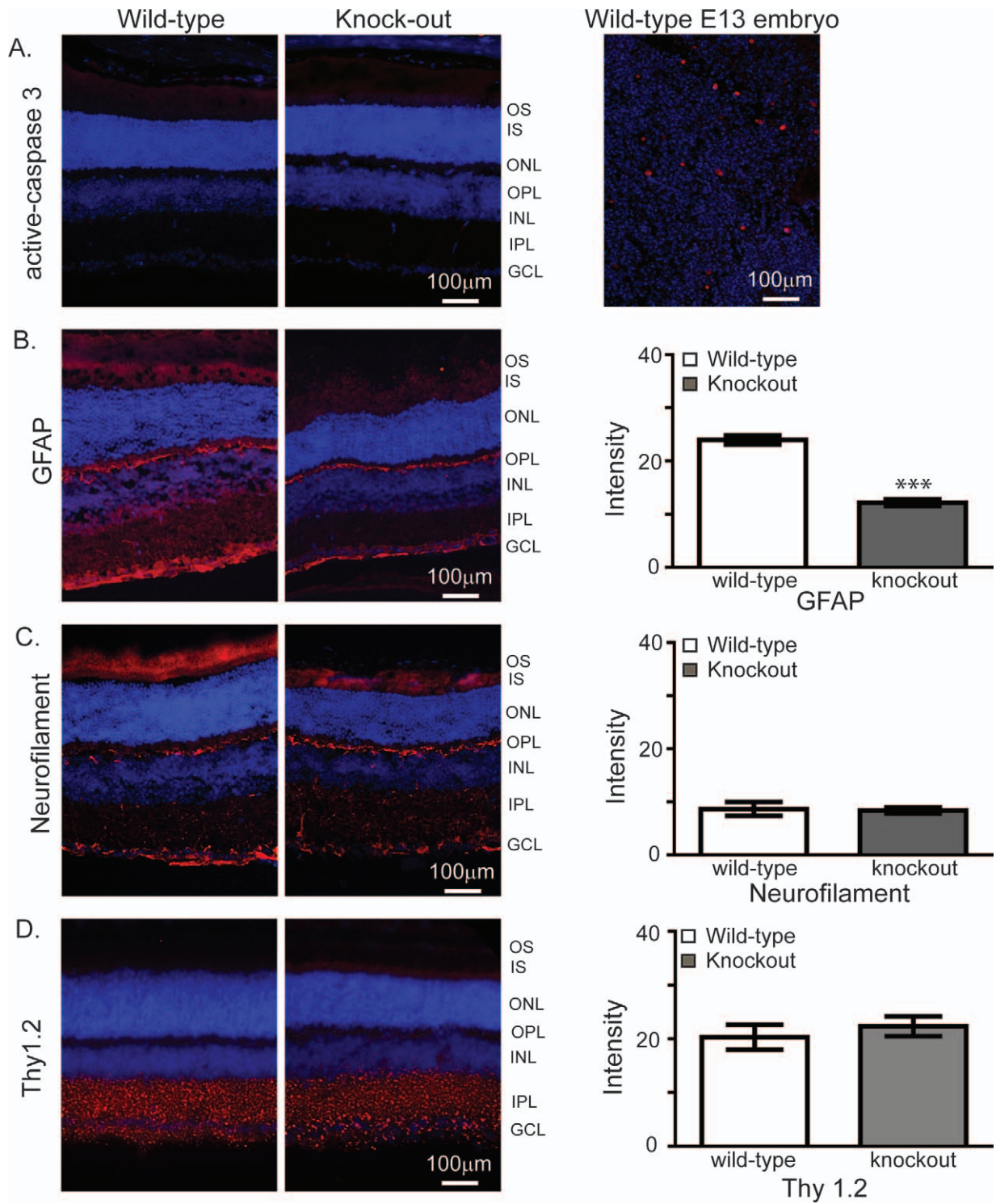


FIGURE 3. In the absence of kl structural proteins are decreased. All IHC representative images are from 7-week-old wild-type or knockout mouse retina. *White bars* denote wild-type and *grey bars* denote knockout quantification. (A) Representative active-caspase 3 expression in retina. Control E13 mouse embryo tissue was processed in parallel and imaged using identical settings. (B) Representative GFAP IHC images and quantification. Quantification of GFAP signal in GCL was conducted across multiple retinas at 7 weeks ($n = 5$ per group, \pm SEM, significance determined by Student's *t*-test: $***P < 0.0001$). (C) Representative neurofilament IHC images and quantification. Quantification of neurofilament signal in OPL was conducted across multiple retinas at 7 weeks ($n = 4$ per group, \pm SEM). (D) Representative Thy1.2 IHC images and quantification. Quantification of Thy1.2 signal in GCL was conducted across multiple retinas at 7 weeks ($n = 4$ per group, \pm SEM).

protein expression in close proximity to but not within the nucleus (Fig. 1C). Relative expression of kl mRNA in retina was compared with the kidney by qPCR, and although clearly detectable by both endpoint PCR and qPCR, kl expression is

much lower in retina than in kidney or brain (Figs. 1D, 1E). Klotho knockouts show signs of neurodegeneration.^{14,17} As such, we probed for retinal degeneration by morphometric analysis of ONL thickness in 7-week-old wild-type and

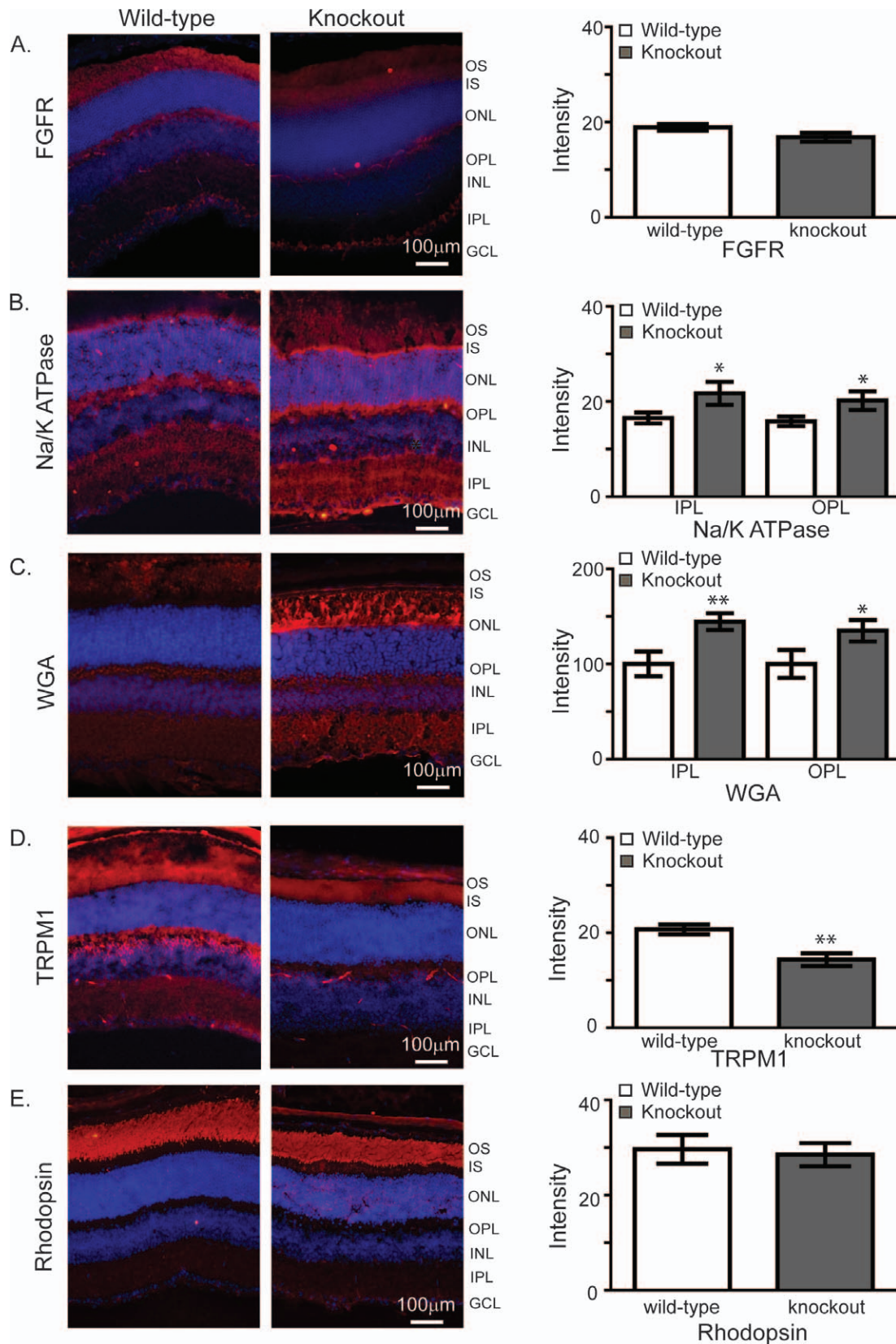


FIGURE 4. In the absence of *kl* ion channel expression is altered. All IHC representative images are from 7-week-old wild-type or knockout mouse retina. *White bars* denote wild-type and *grey bars* denote knockout quantification. (A) Representative FGFR1 IHC images and quantification. No significant difference was observed by quantification of FGFR signal in GCL across multiple retinas at 7 weeks ($n = 4$ per group, \pm SEM). (B) Representative sodium potassium ATPase (NaK ATPase) IHC images and quantification. Quantification of NaK ATPase signal in IPL and OPL was conducted across multiple retinas at 7 weeks ($n = 6$ per group, \pm SEM, significance determined by Student's *t*-test: * $P < 0.04$). (C) Representative

WGA IHC images and quantification. Quantification of WGA signal in IPL and OPL was conducted across multiple retinas at 7 weeks ($n = 7$ per group, \pm SEM, significance determined by Student's *t*-test: $*P < 0.04$, $**P < 0.007$). (D) Representative TRPM1 IHC images and quantification. Quantification of TRPM1 signal in OPL was conducted across multiple retinas at 7 weeks ($n = 4$ per group, \pm SEM, significance determined by Student's *t*-test: $**P < 0.004$). (E) Representative rhodopsin IHC images and quantification. Quantification of the rhodopsin signal in OS was conducted across multiple retinas at 7 weeks ($n = 4$ per group, \pm SEM).

knockout mice. No effect on ONL length or thickness was detected (Fig. 1F).

Absence of *kl* Alters Retinal Protein Expression

In the brain, protein expression and/or localization is altered in *kl* knockouts.¹⁷ Using IHC, and when possible Western blot analysis, changes in both protein expression level and anatomic localization were examined in 7-week-old wild-type or *kl* knockout mice. Synaptic proteins synaptophysin and PSD95 localize to the OPL and IPL.^{20,21} Consistent with results in brain,¹⁷ expression of synaptophysin was significantly lower in both layers of the retina and in retinal lysates in knockout mice (Figs. 2A, 5A). Post synaptic density 95 intensity did not change by IHC where detection was light but retinal lysates reveal an increase in protein expression (Figs. 2B, 5A). Calbindin is a calcium regulating protein primarily expressed in retinal horizontal cells.²² No changes in calbindin-positive

cell number or calbindin total protein was detected (Figs. 2C, 5A). Glutamic acid decarboxylase synthesizes the inhibitory neurotransmitter gamma-aminobutyric acid and is expressed predominantly in OPL and IPL²²; we found GAD67 expression increased in the *kl* knockout OPL and IPL by IHC and Western blotting (Figs. 2D, 5A). Of the proteins examined, synaptophysin and GAD67 showed the largest overall intensity change (Fig. 2). To determine whether the absence of *kl* caused changes in protein expression throughout life, we measured synaptophysin and GAD67 expression in 3-week-old retina. In contrast older animals, no changes in protein expression were observed (Figs. 2A, 2D, striped bars).

In *kl* knockout brain, markers of oxidative stress and apoptosis are increased by 7 weeks of age.^{15,17} In 7-week-old retina, no evidence of photoreceptor degeneration (Fig. 1F), nor increased apoptosis by active-caspase 3 expression (Figs. 3A, 5A) were observed in the *kl* knockout. No changes were

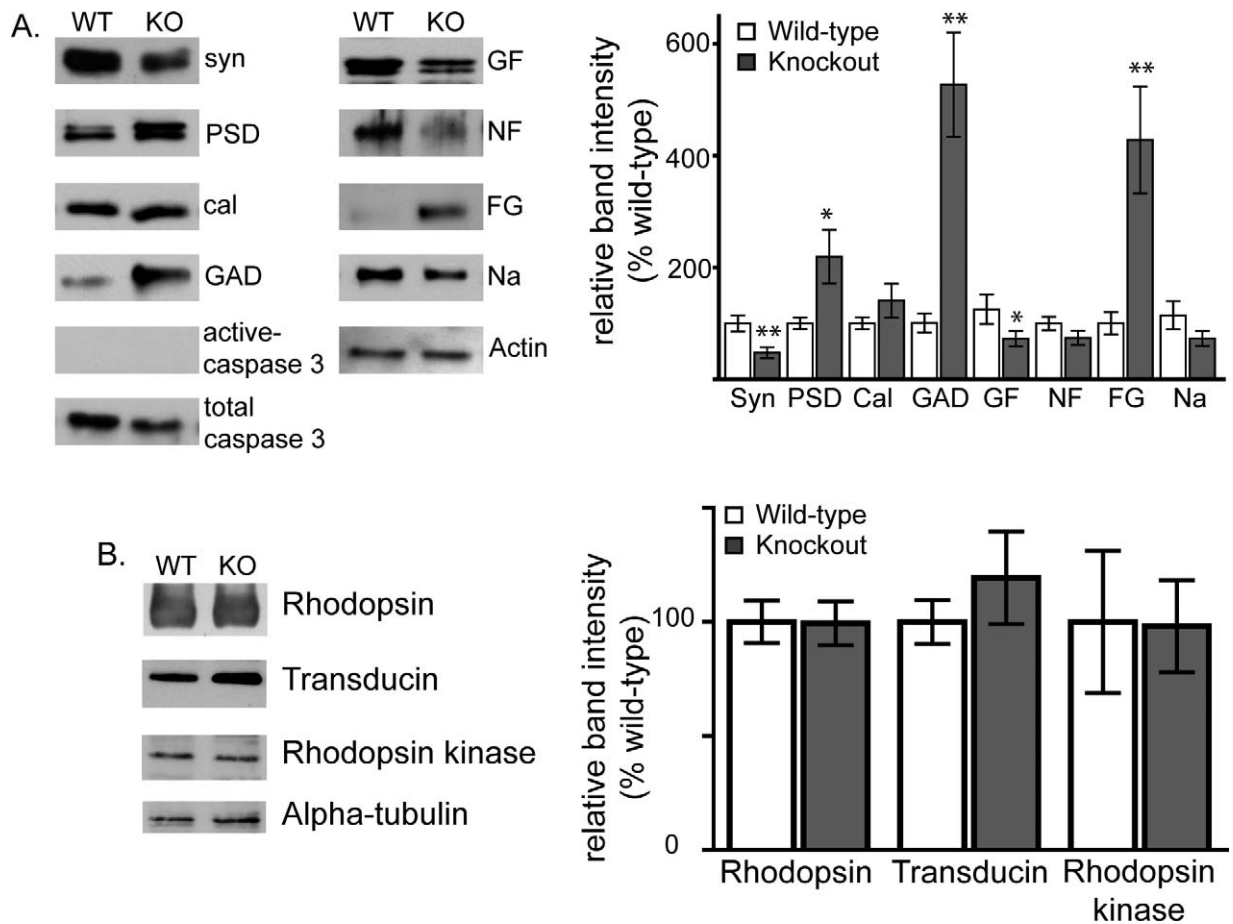


FIGURE 5. The absence of *kl* does not alter expression level of phototransduction proteins. (A) Representative Western blot and quantitation from retinal proteins also studied by IHC. These were: Synaptophysin (syn), PSD95 (PSD), calbindin (cal), GAD67 (GAD), active-caspase 3, total caspase 3, GFAP (GF), neurofilament (NF), FGFR (FG), NaK ATPase (Na). Band intensity was normalized to actin and is represented as a percentage of its relevant wild-type control (wild-type: *white bars*, *kl* knockout: *grey bars*; $n = 4-6$ per group, \pm SEM, significance determined by Student's *t*-test: $*P < 0.05$, $**P < 0.01$). (B) Western blot analysis for phototransduction-related proteins rhodopsin, transducin, and rhodopsin kinase. Band intensity was normalized to actin and is represented as a percentage of its relevant wild-type control (wild-type: *white bars*, *kl* knockout: *grey bars*; $n = 4$ per group, \pm SEM, significance determined by Student's *t*-test).

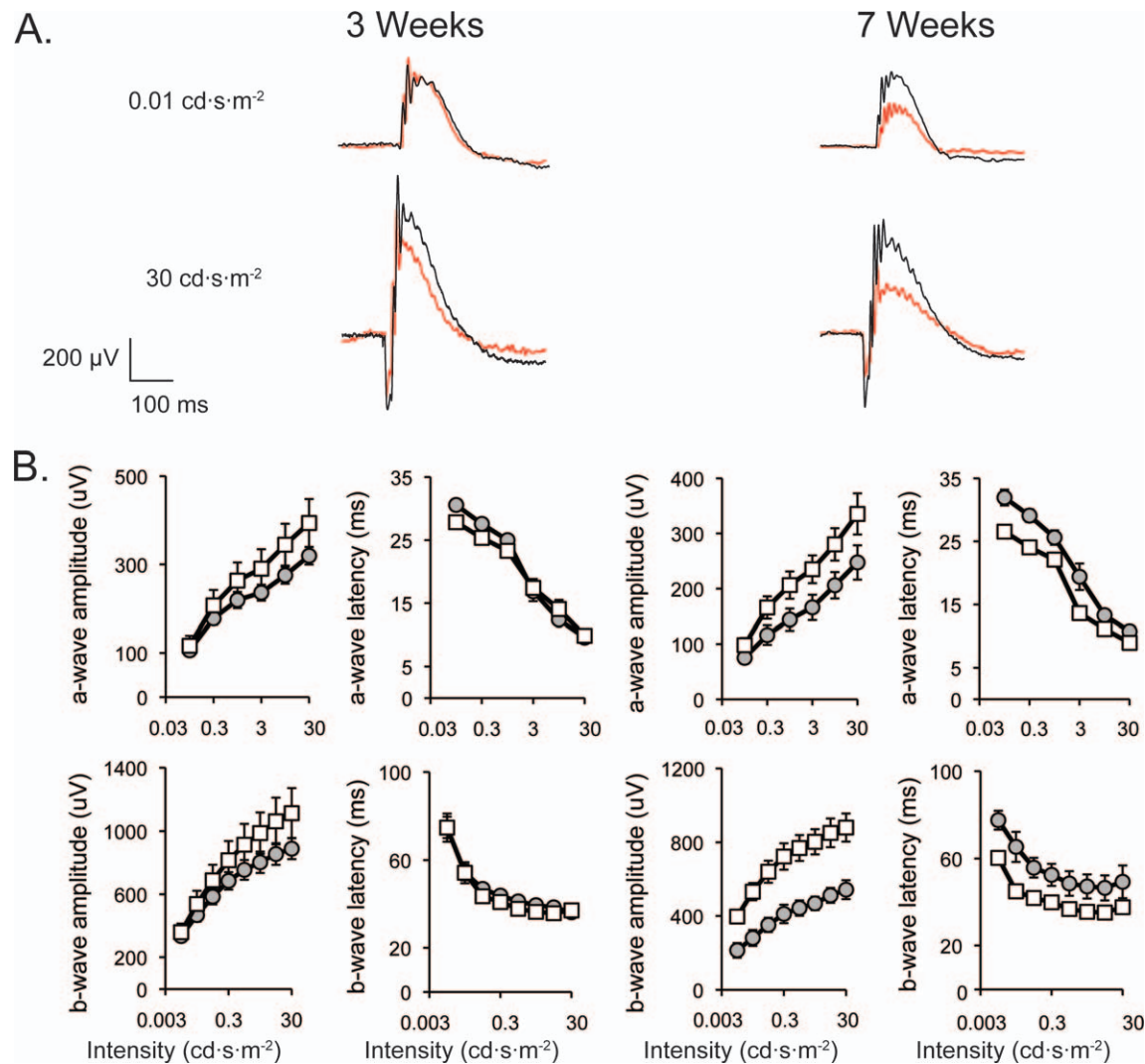


FIGURE 6. Representative scotopic ERG recordings and summary data as a function of flash intensity and age. (A) Overlaid representative scotopic ERG traces at the lowest and highest flash intensities (0.01 and $30 \text{ cd}\cdot\text{s}\cdot\text{m}^{-2}$) from a dark adapted wild-type (*black*) and *kl* knockout (*red*) animal. Electroretinograms were recorded in the same cohort of animals at 3 (*left*) and 7 (*right*) weeks to determine whether the absence of *kl* induces functional changes over time. (B) Summary data averaged across wild-type (*white squares*; $n = 8$; $\pm\text{SEM}$) and *kl* knockout (*grey circles*; $n = 5$; $\pm\text{SEM}$) animals are shown at 3 and 7 weeks of age. a-wave amplitude was measured as baseline to trough, while b-wave amplitude was measured baseline to peak at each flash intensity. Latencies represent time to peak/trough. Klotho knockout a- and b-wave amplitudes and latencies were significantly decreased at 7 weeks of age compared with wild-type controls. Statistical analysis was performed by repeated-measures ANOVA.

observed in expression of SOD, HO-1, or dihydroethidium staining (data not shown).

Structural proteins GFAP and neurofilament are upregulated in *kl* knockout brain.^{17,18} Glial fibrillary acidic protein is expressed in Müller cells in the GCL,²³ and neurofilament is expressed in OPL and GCL.²⁴ Glial fibrillary acidic protein expression decreased by IHC and by Western blot (Figs. 3B, 5A). Neurofilament expression was unchanged in retina (Figs. 3C, 5A), contrasting with brain where its expression was upregulated.¹⁸

Thy1.2 detects a peripheral membrane protein expressed in ganglion cells,^{25,26} where we noted the highest *kl* protein expression (Fig. 1B). No change in Thy1.2 expression was observed (Fig. 3D).

Klotho directly interacts with and modulates the function of both FGFR and sodium/potassium ATPase (Na/K ATPase) in kidney.^{1,27} Although FGFR1 is expressed in retinal ganglion and Müller cells,²⁸ we detected very low level expression by IHC, but retinal lysates indicate an increase in FGFR expression in *kl*

knockout retina (Figs. 4A, 5A). In retina, Na/K ATPase expression is widespread.²⁹ Expression in the *kl* knockout was unchanged in total retinal lysates but increased by IHC (Figs. 4B, 5A). As *kl* directly interacts with Na/K ATPase,²⁷ this difference could be the result of incorrect subcellular distribution in the absence of *kl*.

Klotho removes terminal sialic acid residues on some ion channels, promoting cell surface retention.^{12,30} Wheat germ agglutinin binds to sialic acid and N-acetylglucosamine and was used as a marker of altered sugar modification. Wheat germ agglutinin reactivity was upregulated in IPL of *kl* knockout mice consistent with an increase in sialic acid residues in the absence of *kl* activity (Fig. 4C). In kidney, the sialidase activity of *kl* effects function of transient receptor potential vanilloid (TRPV) channels.^{12,30} Numerous TRP family members are expressed in retina.³¹ We were able to detect TRPM1 expression in IPL consistent with its known localization in bipolar cells.³¹ Retinal expression of TRPM1 was decreased in the IPL of *kl* knockout mice (Fig. 4D).

TABLE. Summary of ERG Results From 3 to 7 Weeks of Age in *kl* Knockout Mice*

	Scotopic				Photopic			
	Wild-Type†	Knockout	Wild-Type	Knockout	Wild-Type	Knockout	Wild-Type	Knockout
Age, wk	3	3	7	7	3	3	7	7
<i>n</i>	11	10	11	6	11	10	11	6
a-wave amplitude max., μ v	393.8 \pm 54.1	319.5 \pm 19.7	335.4 \pm 37.8	247.5 \pm 31.2				
b-wave amplitude max., μ v	1114.0 \pm 156	888.5 \pm 66.1	880.6 \pm 76.5	542.6 \pm 51.2	232.0 \pm 21.1	203.4 \pm 29.8	217.5 \pm 22.5	131.5 \pm 35.6
a-wave/b-wave ratio (%)	35.4%	36.0%	38.1%	45.6%				
A-latency, ms	9.9 \pm 0.3	9.6 \pm 0.2	9.0 \pm 0.3	10.7 \pm 0.3				
B-latency, ms	36.2 \pm 2.4	37.1 \pm 0.9	37.6 \pm 2.8	49.3 \pm 7.5	49.2 \pm 1.7	49.3 \pm 1.3	46.4 \pm 1.9	42.1 \pm 6.4

* Results are the mean \pm SEM.

† *kl* knockout and wild-type controls are 129S1/SvImJ.

As reports vary to whether rhodopsin levels fluctuate in the normal aging retina,^{32,33} we examined rhodopsin levels by IHC and Western blot. No change in rhodopsin expression was observed in *kl* knockout retina (Figs. 4E, 5B). Phototransduction could be affected by changes in retinal proteins; however, the levels of transducin and rhodopsin kinase did not change in *kl* knockout retina (Figs. 5B).

The Absence of *kl* Induces Decreased Retinal Function as Measured by Electroretinography

Wild-type and *kl* knockout mice were dark-adapted and their scotopic, rod dominant ERG responses recorded at 3 and 7 weeks of age. At the 7-week time point, the maximum a-wave amplitude was reduced approximately 26%, and the maximum b-wave amplitude was reduced approximately 38% compared with wild-type controls (Fig. 6, Table). As well, older *kl* knockout animals had slower a- and b-wave latencies (Fig. 6B, Table). Repeated-measures ANOVA analysis was used to determine whether *kl* knockouts showed significant differences in amplitude and latency compared to wild-type controls and whether those changes increased with age. The absence of *kl* resulted in a main effect on scotopic a-wave amplitude ($F_{1,11} = 4.952$, $P = 0.048$); without a significant interaction with age (Fig. 6). In evaluating the scotopic b-wave, the absence of *kl* resulted in a main effect on b-wave amplitude ($F_{1,11} = 10.503$, $P = 0.008$) that also interacted with flash intensity ($F_{1,305,14,357} = 4.382$, $P = 0.046$), but not age (Fig. 6). The absence of *kl* has main effects on scotopic a- and b-wave latency ($F_{1,11} = 15.912$, $P = 0.002$ and $F_{1,11} = 13.156$, $P = 0.004$) that do interact with age ($F_{1,840,20,235} = 3.940$, $P = 0.039$ and $F_{1,696,18,658} = 4.901$, $P = 0.024$) (Fig. 6). Together these data indicate that scotopic a- and b-waves reached peak amplitude more slowly with increasing age in the *kl* knockout mice. The absence of an interaction of genotype with age on a- and b-wave amplitudes implies alterations in retinal function, however small, may be present at 3 weeks of age.

Similar to the scotopic b-wave amplitude, the photopic, cone dominant, ERG responses were measured as the animals aged. By 7 weeks of age, *kl* knockout b-wave amplitude was reduced by approximately 39% (Fig. 7, Table). Using repeated measures ANOVA, the absence of *kl* resulted in a main effect on b-wave amplitude that interacted with flash intensity ($F_{1,13} = 9.019$, $P = 0.010$ and $F_{1,197,15,563} = 9.085$, $P = 0.006$), but not age (Fig. 7). Photopic b-wave latency was unaffected ($P > 0.05$, Fig. 7). As measured by changes in both scotopic and photopic ERG, the *kl* knockout mice experience a severe loss of retinal function over their lifespan.

DISCUSSION

We report the expression of *kl* mRNA and protein in mouse retina. Loss of *kl* in knockout animals results in changes in protein expression and a decrease in retinal function. Although changes in retinal function were not observed at 3 weeks, as animals continued to age retinal function dramatically decreased. Although no retinal degeneration was detectable, decreased a- and b-amplitudes and alterations in synaptic function represented by increased a- and b-wave latency were observed. Commiserate with changes in function at 7 weeks of age, protein expression changes were observed in markers of synaptic function with a decrease in synaptophysin and an increase in GAD67. This suggests a shift in the excitation/inhibition balance in older knockouts towards increased inhibition and may explain the slower a- and b-waves. Fibroblast growth factor receptor and sodium potassium ATPase (NaK ATPase) upregulation and TRPM1 downregulation were noted indicating homeostatic disruptions across layers of the retina. *Klotho* modulates ion channel activity both through direct interactions and through its activity as a sialidase.^{1,12,30} *Klotho* does not appear to be a nuclear protein, but is found adjacent to the nucleus in the soma (Fig. 1C). The absence of *kl* resulted in increased WGA binding, suggesting altered sugar modifications that could induce changes in ion flux from plasma membrane resident ion channels similar to those observed with kidney TRPV and renal outer medullary potassium channels.^{12,30} The increased WGA staining indicates potential dysfunction throughout all layers of retina. Interestingly, absence of *kl* was not associated with ganglion cell loss (Fig. 3D) but with lower levels of GFAP immunoreactivity (Fig. 3B), possibly weakening the structural integrity of the inner retina in the *kl* knockout animals.

In the retina, we report decreased a- and b-wave amplitudes along with a progressive age-related increase in latency in a- and b-waves (Fig. 6). Importantly, these changes in function are not accompanied by evidence of retinal degeneration as measured by cell loss/death (Figs. 1, 3, 5) or loss of phototransduction proteins (Figs. 4E, 5B). Thus, the *kl* knockout mouse does appear to represent an accelerated retinal aging model as changes by 7 weeks of age are consistent with a healthy mouse retina at 1 year.³² However, while decreased a- and b-wave amplitude is a consistent feature in aging studies,^{32,33} reports of changes in latency and evidence of degeneration are inconsistent. Examining the effect of aging between C57BL/6 and BALB/c mouse strains at 1 and 17 months, ERG amplitudes decreased without changes in latency.³² Retinal thickness and rhodopsin content also decreased with age.³²

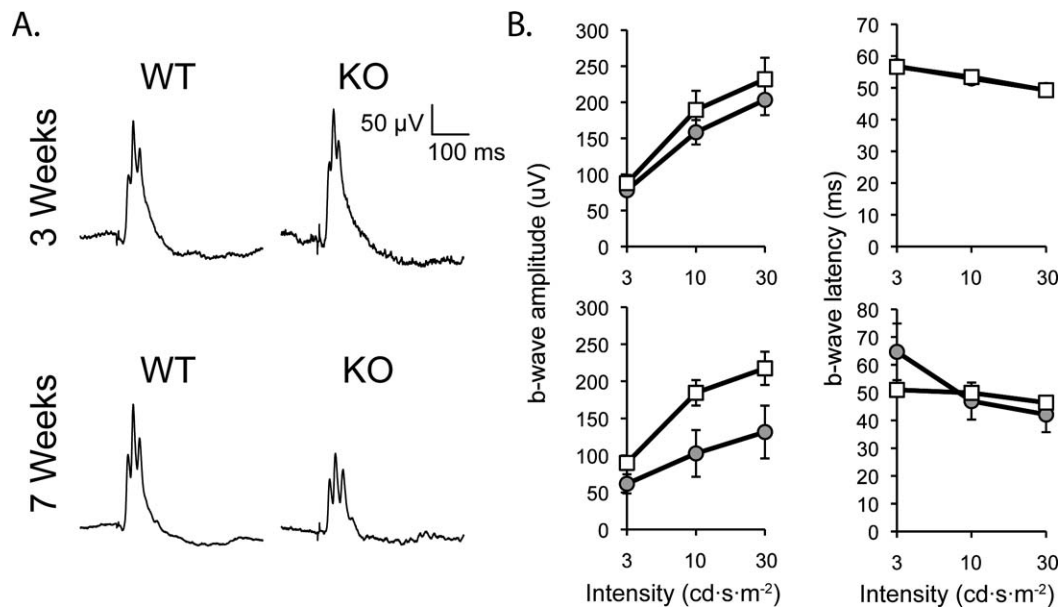


FIGURE 7. Photopic ERG responses are also decreased in *kl* knockout mice. (A) Representative photopic ERG recordings from 3 (*top row*) and 7 (*bottom row*) week-old wild-type and *kl* knockout animals. (B) Summary data averaged across wild-type (*white squares*; $n = 9$; \pm SEM) and *kl* knockout (*grey circles*; $n = 6$; \pm SEM) animals at 3 (*top row*) and 7 (*bottom row*) weeks of age. Klotho knockout b-wave amplitude (baseline to peak) and was significantly decreased at 7 weeks of age. Statistical analysis was performed by repeated-measures ANOVA.

In addition to an aging phenotype, functional deficits in our study are similar to those in the IGF-1 knockout mouse where a- and b-wave amplitude progressively decline.³⁴ In this mouse, changes in function are attributed to altered synaptic function.³⁴ Klotho knockout mice are hypoglycemic and sensitive to insulin/IGF-1, indicative of a role for *kl* in insulin signaling inhibition.³⁵ It is possible that effects mediated by the absence of *kl* in retina are the result of changes in insulin signaling that critically underlie healthy retinal function. Changes in the *kl* knockout ERG are also similar to those observed in the DBA/2J model of glaucoma.³⁶

Recent work from Farinelli and colleagues³⁷ showed upregulation of *kl* protein expression in dying cells in models of retinal degeneration. Organotypic explant cultures of wild-type retina exposed to recombinant *kl* protein displayed greater nuclear disorganization than controls.³⁷ These results would suggest that *kl* is involved in disease states as well as normal function, however whether it is causal in disease development is unknown. In contrast to our findings, *kl* protein expression was not detected in wild-type retina although different antibodies were utilized between studies.³⁷

A potential confounding factor to interpretation of our data is the profound dysfunction in nearly every organ system caused by the systemic absence of *kl*. As such, the changes observed in retina could be the result of toxicity and not a direct effect of *kl*. Changes in protein expression were not uniform and cell death was not observed (Figs. 2–5), reducing the likelihood that systemic toxicity accounts for all observed changes. Further study of this phenomenon would benefit from a retina specific knockout of *kl*. The presence of normal *kl* function in the kidney would eliminate many of the systemic toxic effects and allow observation of the result of the loss of *kl* in retina over a longer time course. As the profound functional deficit noted here may be anticipated to cause retinal degeneration in a longer-lived animal, a retinal specific *kl* knockout would test the hypothesis that retinal degeneration would be a consequence of the aberrant electrical signaling seen in *kl* knockout animals.

Acknowledgments

The authors thank McGinty Chilcutt, Dominique Tull, Chelsea McCoy, and Stephen J. Mehi for experimental assistance. Appreciation is also extended to the University of Alabama at Birmingham (UAB) Neuroscience Core (P30-NS047466) for tissue processing, and the UAB Vision Science Research Core for electroretinogram instrumentation (P30 EY003039).

Supported by grants from the University of Alabama at Birmingham Medical Scientist Training Program T32 GM008361 (NJR), National Institutes of Health (NIH)/National Eye Institute (NEI) RO1 EY019311 (AKG), E. Matilda Ziegler Foundation for the Blind (AKG), and NIH/NIA R00 AG034989 (GDK).

Disclosure: **N.J. Reish**, None; **A. Maltare**, None; **A.S. McKeown**, None; **A.M. Laszczyk**, None; **T.W. Kraft**, None; **A.K. Gross**, None; **G.D. King**, None

References

- Kurosu H, Ogawa Y, Miyoshi M, et al. Regulation of fibroblast growth factor-23 signaling by klotho. *J Biol Chem.* 2006;281:6120–6123.
- Yamamoto M, Clark JD, Pastor JV, et al. Regulation of oxidative stress by the anti-aging hormone klotho. *J Biol Chem.* 2005;280:38029–38034.
- Kuro-o M, Matusumura Y, Aizawa H, et al. Mutation of the mouse klotho gene leads to a syndrome resembling ageing. *Nature.* 1997;390:45–51.
- Brownstein CA, Adler F, Nelson-Williams C, et al. A translocation causing increased alpha-klotho level results in hypophosphatemic rickets and hyperparathyroidism. *Proc Natl Acad Sci U S A.* 2008;105:3455–3460.
- Ichikawa S, Imel EA, Kreiter ML, et al. A homozygous missense mutation in human KLOTHO causes severe tumoral calcinosis. *J Clin Invest.* 2007;117:2684–2691.
- Kuro-o M. Klotho and aging. *Biochim Biophys Acta.* 2009;1790:1049–1058.
- Duce JA, Podvin S, Hollander W, et al. Gene profile analysis implicates Klotho as an important contributor to aging

- changes in brain white matter of the rhesus monkey. *Glia*. 2008;56:106-117.
8. Kato Y, Arakawa E, Kinoshita S, et al. Establishment of the anti-Klotho monoclonal antibodies and detection of Klotho protein in kidneys. *Biochem Biophys Res Commun*. 2000;267:597-602.
 9. Doi S, Zou Y, Togao O, et al. Klotho inhibits transforming growth factor-beta1 (TGF-beta1) signaling and suppresses renal fibrosis and cancer metastasis in mice. *J Biol Chem*. 2011;286:8655-8665.
 10. Kurosu H, Yamamoto M, Clark JD, et al. Suppression of aging in mice by the hormone Klotho. *Science*. 2005;309:1829-1833.
 11. Liu H, Fergusson MM, Castilho RM, et al. Augmented Wnt signaling in a mammalian model of accelerated aging. *Science*. 2007;317:803-806.
 12. Cha SK, Ortega B, Kurosu H, et al. Removal of sialic acid involving Klotho causes cell-surface retention of TRPV5 channel via binding to galectin-1. *Proc Natl Acad Sci U S A*. 2008;105:9805-9810.
 13. Li SA, Watanabe M, Yamada H, et al. Immunohistochemical localization of Klotho protein in brain, kidney, and reproductive organs of mice. *Cell Struct Funct*. 2004;29:91-99.
 14. Kosakai A, Ito D, Nihei Y, et al. Degeneration of mesencephalic dopaminergic neurons in klotho mouse related to vitamin D exposure. *Brain Res*. 2011;1382:109-117.
 15. Nagai T, Yamada K, Kim HC, et al. Cognition impairment in the genetic model of aging klotho gene mutant mice: a role of oxidative stress. *FASEB J*. 2003;17:50-52.
 16. Park SJ, Shin EJ, Min SS, et al. Inactivation of JAK2/STAT3 signaling axis and downregulation of M1 mAChR cause cognitive impairment in klotho mutant mice, a genetic model of aging. *Neuropsychopharmacology*. 2013;38:1426-1437.
 17. Shiozaki M, Yoshimura K, Shibata M, et al. Morphological and biochemical signs of age-related neurodegenerative changes in klotho mutant mice. *Neuroscience*. 2008;152:924-941.
 18. Uchida A, Komiya Y, Toshiro T, et al. Neurofilaments of Klotho, the mutant mouse prematurely displaying symptoms resembling human aging. *J Neurosci Res*. 2001;64:364-370.
 19. German DC, Khobahy I, Pastor J, Kuro OM, Liu X. Nuclear localization of Klotho in brain: an anti-aging protein. *Neurobiol Aging*. 2012;33:1483.e25-30.
 20. Kihara AH, Santos TO, Paschon V, Matos RJ, Britto LR. Lack of photoreceptor signaling alters the expression of specific synaptic proteins in the retina. *Neuroscience*. 2008;151:995-1005.
 21. Koulen P, Fletcher EL, Craven SE, Bredt DS, Wassle H. Immunocytochemical localization of the postsynaptic density protein PSD-95 in the mammalian retina. *J Neurosci*. 1998;18:10136-10149.
 22. Deniz S, Wersinger E, Schwab Y, et al. Mammalian retinal horizontal cells are unconventional GABAergic neurons. *J Neurochem*. 2011;116:350-362.
 23. Wu KH, Madigan MC, Billson FA, Penfold PL. Differential expression of GFAP in early v late AMD: a quantitative analysis. *Br J Ophthalmol*. 2003;87:1159-1166.
 24. Bromberg JS, Schachner M. Localization of nervous system antigens in retina by immunohistology. *Invest Ophthalmol Vis Sci*. 1978;17:920-924.
 25. Guy J, Qi X, Koilkonda RD, et al. Efficiency and safety of AAV-mediated gene delivery of the human ND4 complex I subunit in the mouse visual system. *Invest Ophthalmol Vis Sci*. 2009;50:4205-4214.
 26. Huang X, Wu DY, Chen G, Manji H, Chen DF. Support of retinal ganglion cell survival and axon regeneration by lithium through a Bcl-2-dependent mechanism. *Invest Ophthalmol Vis Sci*. 2003;44:347-354.
 27. Imura A, Tsuji Y, Murata M, et al. alpha-Klotho as a regulator of calcium homeostasis. *Science*. 2007;316:1615-1618.
 28. Catalani E, Tomassini S, Dal Monte M, Bosco L, Casini G. Localization patterns of fibroblast growth factor 1 and its receptors FGFR1 and FGFR2 in postnatal mouse retina. *Cell Tissue Res*. 2009;336:423-438.
 29. Arakaki X, McCleary P, Tachy M, et al. Na, K-ATPase alpha isoforms at the blood-cerebrospinal fluid-trigeminal nerve and blood-retina interfaces in the rat. *Fluids Barriers CNS*. 2013;10:14.
 30. Cha SK, Hu MC, Kurosu H, et al. Regulation of renal outer medullary potassium channel and renal K(+) excretion by Klotho. *Mol Pharmacol*. 2009;76:38-46.
 31. Gilliam JC, Wensel TG. TRP channel gene expression in the mouse retina. *Vision Res*. 2011;51:2440-2452.
 32. Gresh J, Goletz PW, Crouch RK, Rohrer B. Structure-function analysis of rods and cones in juvenile, adult, and aged C57Bl/6 and Balb/c mice. *Vis Neurosci*. 2003;20:211-220.
 33. Li C, Cheng M, Yang H, Peachey NS, Naash MI. Age-related changes in the mouse outer retina. *Optom Vis Sci*. 2001;78:425-430.
 34. Rodriguez-de la Rosa L, Fernandez-Sanchez L, Germain F, et al. Age-related functional and structural retinal modifications in the Igf1-/- null mouse. *Neurobiol Dis*. 2012;46:476-485.
 35. Utsugi T, Ohno T, Ohyama Y, et al. Decreased insulin production and increased insulin sensitivity in the klotho mutant mouse, a novel animal model for human aging. *Metabolism*. 2000;49:1118-1123.
 36. Harazny J, Scholz M, Buder T, Lausen B, Kremers J. Electrophysiological deficits in the retina of the DBA/2J mouse. *Doc Ophthalmol*. 2009;119:181-197.
 37. Farinelli P, Arango-Gonzalez B, Volkl J, et al. Retinitis pigmentosa: over-expression of anti-ageing protein Klotho in degenerating photoreceptors [published online ahead of print June 24, 2013]. *J Neurochem*. doi:10.1111/jnc.12353.